Post-treatment MRI findings of hepatocellular carcinoma

Esra Özkavukcu, Nuray Haliloğlu, Ayşe Erden

ABSTRACT

In addition to surgery, ablative and transarterial therapies are widely accepted treatment options for hepatocellular carcinoma. Although post-treatment follow-up is usually done with both computed tomography and magnetic resonance imaging (MRI), MRI is found to be superior in detecting residual or recurrent tumors after treatment. Familiarity with post-treatment MRI findings is critical for the correct interpretation of these examinations, and for guiding further therapies.

Key words: • hepatocellular carcinoma • radiofrequency ablation • magnetic resonance imaging

Hepatocellular carcinoma (HCC) is one of the most common cancers worldwide, and has a poor prognosis unless treated. In patients with unresectable tumors, the median survival is less than four months, whereas in patients with less-advanced disease survival is less than one year if left untreated (1).

Generally, surgical resection is the gold standard therapy for HCC, and has been proven to provide long-term survival in large, prospective trials (1). Unfortunately, more than 80% of patients with HCC have underlying cirrhosis, and only 10–15% of HCC patients are eligible for liver resection due to the severity of underlying cirrhosis or the diffuse distribution of the tumor (2). Another treatment option is liver transplantation. It is theoretically the best treatment for HCC as it not only provides the widest possible resection margins, but also removes the remaining diseased and nonfunctional liver tissue that is at risk for the development of de novo cancer. In addition, in contrast to surgical resection, hepatic function is restored following transplantation (1, 3).

Except for patients who have a suitable donor for living donor transplantation, the shortage of donor organs is the main problem that makes transplantation less available to patients awaiting transplantation. Moreover, orthotopic liver transplantation results in approximately 15% 1-year mortality for adults. Therefore, transplantation may not be appropriate for early cancers that have a better prognosis (3).

Currently, ablative therapies are the second choice for patients with liver tumors who are not eligible for surgery (because of advanced liver disease, or because of the location of the tumor). Local ablation also may be used to control HCC while awaiting transplantation (3). These therapies are known to have low morbidity and mortality, as well as being less expensive than surgical resection. Other advantages of ablative therapies compared with surgery include the possibility of real-time imaging guidance, and the ability to perform these procedures on outpatients (4).

Other treatment options for patients with unresectable HCCs are transarterial chemoembolization (TACE) or transarterial radioembolization (using yttrium-90 microspheres). These transarterial therapies are based on the idea that HCC is supplied mainly by the hepatic artery. TACE causes a cytotoxic effect on malignant cells, as well as obliteration of the feeding arteries of the tumor (5). Metastases from colon cancer and neuroendocrine tumors also can be treated using this method (5).

Besides detecting and diagnosing the HCC lesions, contrast enhanced computed tomography (CT) and magnetic resonance imaging (MRI) are widely used in the post-treatment follow-up of these patients, for the detection of residual or recurrent tumors after treatment, as well as for the depiction of post-treatment complications. The early detection of residual or recurrent tumor is important for planning new interventions (5). There is suggestive evidence that MRI is more accurate than other ra-

From the Department of Radiology (E.Ö. ✉ eozkavukcu@gmail.com), Ankara University School of Medicine, Ankara, Turkey.
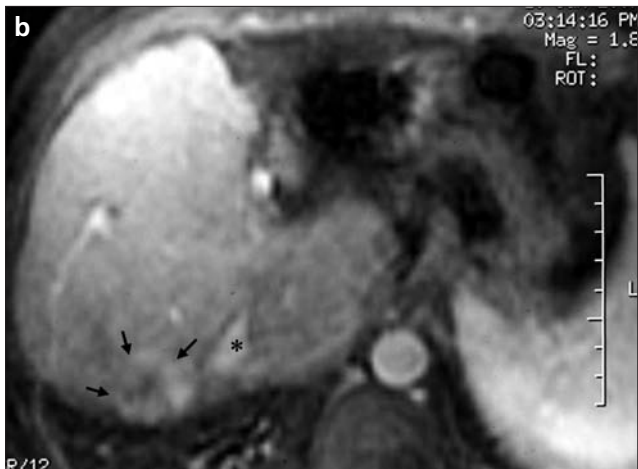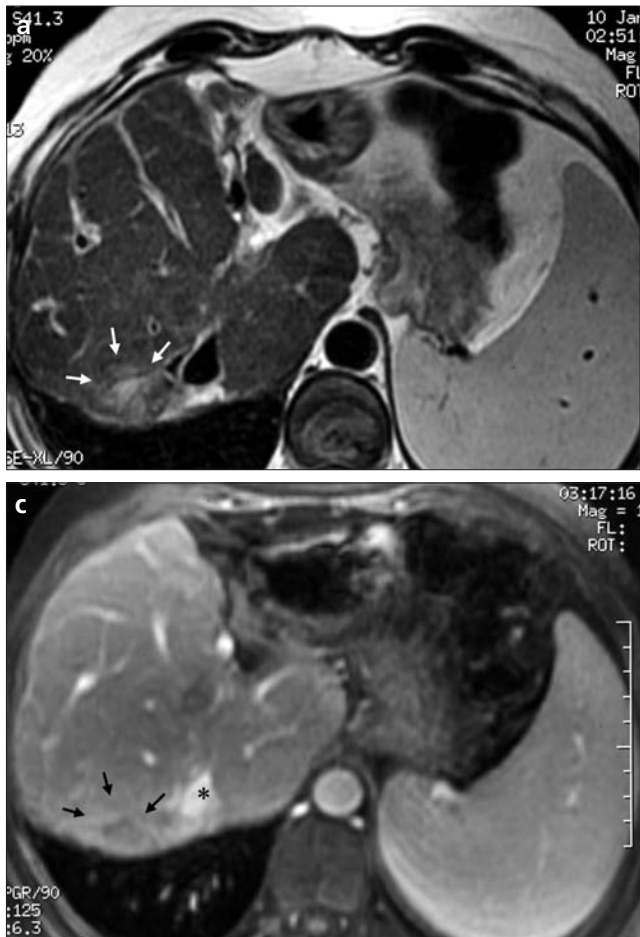
Figure 1. a–c. Postoperative axial MR images of a 44-year-old woman with hepatocellular carcinoma. T2-weighted MR image (**a**) shows a heterogeneous-hyperintense area *(white arrows)* compared with the liver parenchyma, adjacent to the resection site at segment 7 of the liver. On portal (**b**) and late (**c**) phase postcontrast MR sequences, a temporary and slightly heterogeneous enhancing area at the resection site can be seen on the portal phase (**b**) which is less prominent (almost disappeared) on the late phase image (*black arrows in* **b** *and* **c**). T2-signal intensity and enhancement pattern was not typical for residual or recurrent tumor. Subsequent follow-up MR studies (not shown), did not show recurrent disease at the resection site. (Asterisk, inferior vena cava.)

diological modalities in the detection of residual or recurrent tumors (5). Preliminary studies are being conducted to assess the role of diffusion-weighted MRI and MR spectroscopy in addition to conventional MRI in evaluating tumor response after locoregional therapies (6).

Herein, we present a review of the literature on MRI findings following various treatment procedures for HCC lesions. MRI findings following liver transplantation will not be discussed here, as it is beyond the scope of this review. Also, MRI findings after radioembolization will not be examined, as follow-up studies after this treatment method are routinely performed with CT or positron emission tomography in our institution.

1. Surgical resection

Liver resection has some disadvantages compared with transplantation, i.e., not eliminating the remaining portions of liver at risk for de novo malignancy, and not improving hepatic function; however, for a patient with a non-cirrhotic liver with a resectable tumor (or tumors) and no evidence of vascular invasion or extrahepatic spread, resection is still the treatment of choice (3).

Partial hepatectomy causes damage along the resection margin as is reflected by focal areas of edema and granulation (5). Moreover, following partial hepatectomy, there may be tissue damage or a circulatory disorder in the liver. Local vascular damage due to partial hepatectomy and surgical manipulation, or physical tissue restoration following partial hepatectomy, or post-operative complications can result in portal/hepatic venous obstruction or arterioportal shunts (7).

In a study of 30 patients who had undergone partial hepatectomy, Goshima et al. found a total of 39 early-enhancing non-neoplastic lesions, which were circular, oval, irregular, wedge-shaped, or serpiginous, and were located along the liver edge or near the resection area (Fig. 1) (7). Thirty six per cent of these pseudolesions appeared slightly hyperintense on T2-weighted images (Fig. 1a). Although these pseudolesions showed enhancement on hepatic arterial phase images, they did not appear hypointense on portal venous-, or equilibrium-phase images (Fig. 1c). Moreover, these non-neoplastic areas resolved on follow-up studies (7).

Residual or recurrent HCC lesions usually have MRI appearance similar to that of the pre-treatment HCC lesions. Thus, in contrast to the aforementioned non-neoplastic and temporary enhancing areas, residual or recurrent HCC lesions tend to show washout on portal or late phase postcontrast MR images (5).

2. Ablative therapies

Ablative techniques can be classified as either chemical or thermal (physical) (3). Chemical ablation refers to the use of ethanol and acetic acid, whereas thermal ablation is achieved by using heat (radiofrequency [RF] ablation, microwave ablation, laser ablation); or cold (cryoablation) (5, 8). Among all the ablative techniques, RF ablation is the one most widely used for both primary and secondary malignances of the liver (5, 9, 10), but all techniques produce coagulation necrosis, and demonstrate similar imaging features on follow-up studies (4, 10). Furthermore, innovations to increase energy

deposition, such as the use of internal cooling, or the biophysical limitations of thermal ablation, such as the effect of tissue blood flow that limits coagulation, apply equally to all ablative methods (4).

2.a. Radiofrequency (RF) ablation

RF ablation is a well-tolerated (3, 11, 12) and effective method in the local control of hepatic tumors (13). In general, patient inclusion criteria for RF ablation require few (<5), and small (<3 cm) lesions without extrahepatic disease (6). RF ablation can be performed percutaneously under ultrasonographic guidance, using local anesthesia. It may also be performed at laparoscopy or laparotomy. This method causes focal coagulative necrosis of hepatic tumors by producing thermal energy using an alternating electric current generator at a radiofrequency of 200–1,200 kHz (1). Increased thermal effect results not only in denaturation of structural proteins, but also in degradation of enzymatic proteins. Coagulative necrosis is a type of necrosis in which the affected cells or tissue are converted to a dry, dull, fairly homogeneous eosinophilic mass without nuclear staining, as a result of the coagulation of protein, as may occur in an infarct. It may be caused by heat, ischemia, and other agents that destroy tissue.

After RF ablation, the postprocedure necrotic cavity must exceed the tumor margins by 0.5 to 1 cm (12). The ablation of adjacent liver parenchyma enables the eradication of microscopic tumor foci at the tumor boundary, as tumor cells often infiltrate into this region (5, 10).

Familiarity with post-RF ablation MRI findings is crucial for the accurate interpretation of these examinations. In the early post-ablation period (up to one week after ablation), the necrotic cavity shows variable signal intensity changes on T1- and T2-weighted sequences (5). Variability in T1- and T2-signal intensity of the necrotic cavity may mask residual tumors. Thus, contrast-enhanced MRI must be performed for accurate analysis, because it is difficult to interpret unenhanced MRIs in this early period (14).

Small fluid collections (sub-phrenic, sub-hepatic, sub-capsular) may be seen in the early post-ablation period (5, 10). Also, gas bubbles may be seen in the ablation zone, which should disappear within a few days (10). Gas bubbles appear as signal-void round areas on both T1- and T2-weighted images.

Perfusion abnormality (wedge-shaped enhancement of the liver parenchyma adjacent to the ablation zone on arterial phase images) is also a temporary and early finding following ablative therapies (5, 6, 13). This is probably due to peripheral arterioportal shunts caused by the needle puncture and/or thermal damage. Perfusion abnormalities usually vanish by 30 days after the procedure (6).

In addition, a thin rim surrounding the necrotic cavity can be seen in the early period. This rim has low signal intensity on T1-, and high signal intensity on T2-weighted images (6, 14, 15) (Figs. 2a, b). The histologic analysis of the perilesional rim reveals a vascularized inflammatory reaction, hemorrhage, and granulation tissue (12). This perilesional rim shows moderate to intense enhancement on arterial-dominant phase images (14). The thickness and enhancement of this rim regress progressively, and it generally disappears by six months after ablation (5, 15). Dromain et al. reported that this thin (usually 1 mm) and regular rim, which enhances progressively after contrast injection, was present at two months in 32% of the total RF-ablated areas (13). They suggested that the rim is better seen at later phases of post-contrast images. This enhancing rim should not be confused with peripheral tumor regrowth (13, 15). With residual tumor or recurrence of the tumor, the area of contrast enhancement is irregular and thicker (13, 15). Additionally, an ill-defined perilesional enhancement can be seen on arterial-phase images, reflecting inflammatory changes, which also gradually disappear in 3 to 6 months following therapy (5).

The necrotic cavity does not show enhancement on postcontrast images (4–6) (Figs. 2c, d). T1-signal intensity is determined by the stage of the hemorrhage, whereas T2-signal intensity depends on the presence of coagulative, or liquefactive necrosis (14). Liquefactive necrosis partly or completely consists of fluid remnants of tissue that became necrotic and was digested by enzymes. Because of the fluid content, liquefactive necrosis appears hyperintense, while coagulative necrosis appears hypointense on T2-weighted MR images (5) (Fig. 3).

Dromain et al. also noted that later, at 2 months after RF therapy, most RF-treated areas were hyperintense on T1-weighted (due to hemorrhage or proteinaceous material), and hypointense on T2-weighted images (coagulative necrosis) (Figs. 2a, b) (13). This uniform hypointensity on T2-weighted images, and the lack of enhancement of the RF-treated area on post-contrast images (Figs. 2c, d), always corresponded to effective treatment (13). However, in 14% of the successfully treated lesions, marked T2-hyperintensity was encountered, probably signifying biloma or liquefactive necrosis (Fig. 3b). Residual tumor always shows a less intense (moderate) T2-intensity (13).

The probe track usually is observed as a linear parenchymal defect extending from the liver surface into the post-ablation cavity. The track is hypointense on both T1- and T2-weighted MR images, and does not show enhancement on post-contrast series. Yet, the liver parenchyma surrounding the probe track may show some enhancement because of edema and inflammation (5).

Other ancillary MRI findings after RF ablation therapy include segmental intrahepatic biliary duct dilatation which is seen upstream to the ablation zone, and ipsilateral pleural effusion (15).

In patients treated successfully with ablative therapies, the ablated zone either remains with similar immediate post-therapy dimensions, or shrinks in size (Fig. 4). The duration of shrinkage depends on the kind of therapy used and the presence of underlying liver disease, and is usually completed within 6 to 12 months of ablation (5). Moreover, small necrotic cavities may look like focal hepatic atrophy with capsule retraction, or may disappear completely (5, 6). The postablative coagulation area following RF ablation shrinks more slowly than does that resulting from ethanol injection (13).

Long-term evaluation of follow-up imaging (>4–6 months) is generally easier than is evaluation in the immediate imaging following ablation, because the inflammation is resolved. On MRI, the ablation area shows more homogeneous T1-hyperintense and T2-hypointense signal (14). Thus, the depiction of residual tumor becomes easier by the distinction between the moderately hy-
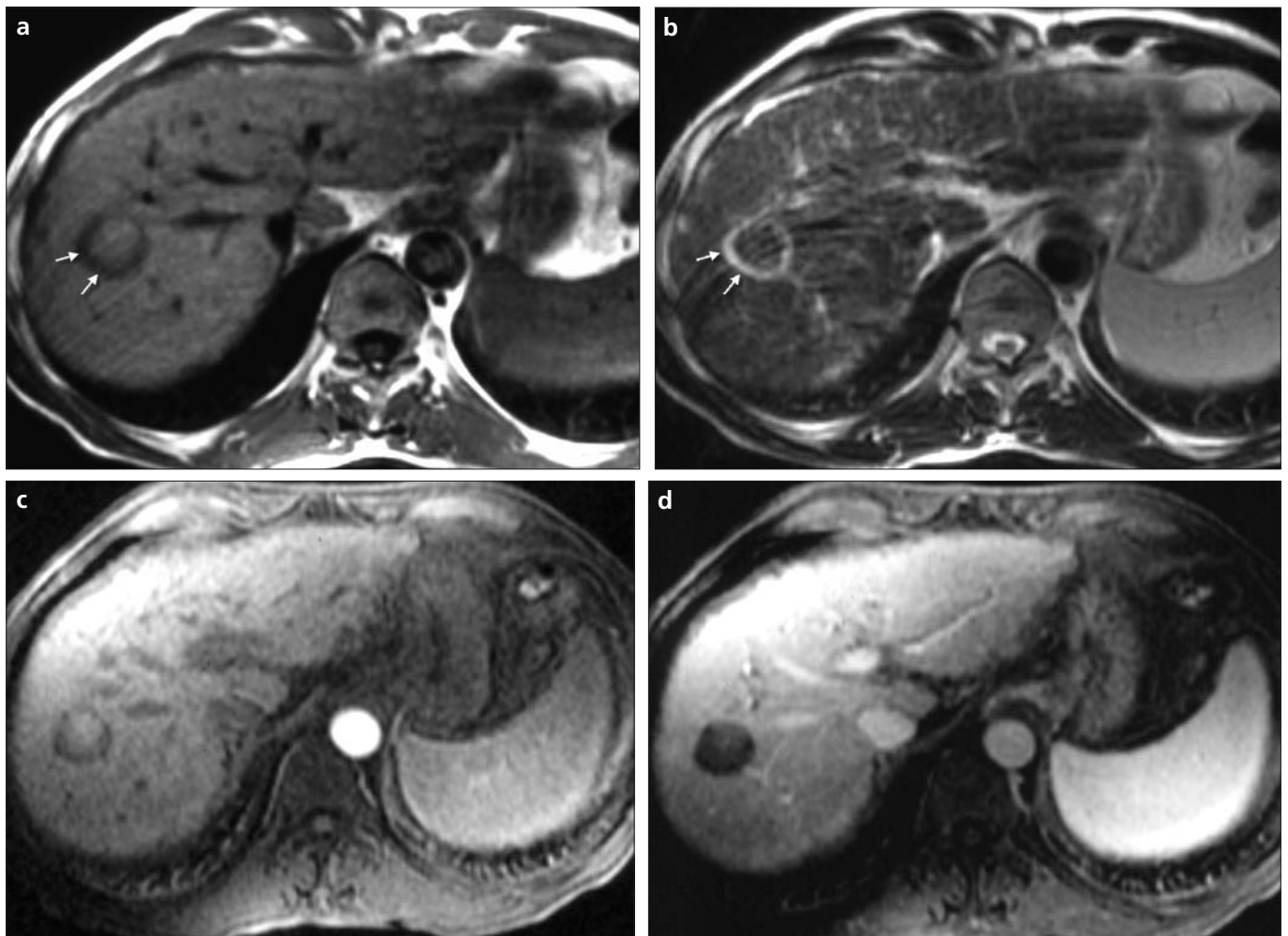
Figure 2. a–d. Axial T1-weighted **(a)**, T2- weighted **(b)**, postcontrast arterial **(c)**, and late phase **(d)** MR images of a 50-year-old man following successful radiofrequency ablation therapy for hepatocellular carcinoma. A T1-hypointense, T2-hyperintense perilesional rim surrounding the necrotic cavity is evident (*arrows in* **a** *and* **b**). The necrotic cavity does not show enhancement following the administration of contrast material **(c, d)**. Note that the hyperintensity of the necrotic cavity seen at the arterial phase is due to the hemorrhagic content of the cavity, rather than contrast enhancement **(c)**.
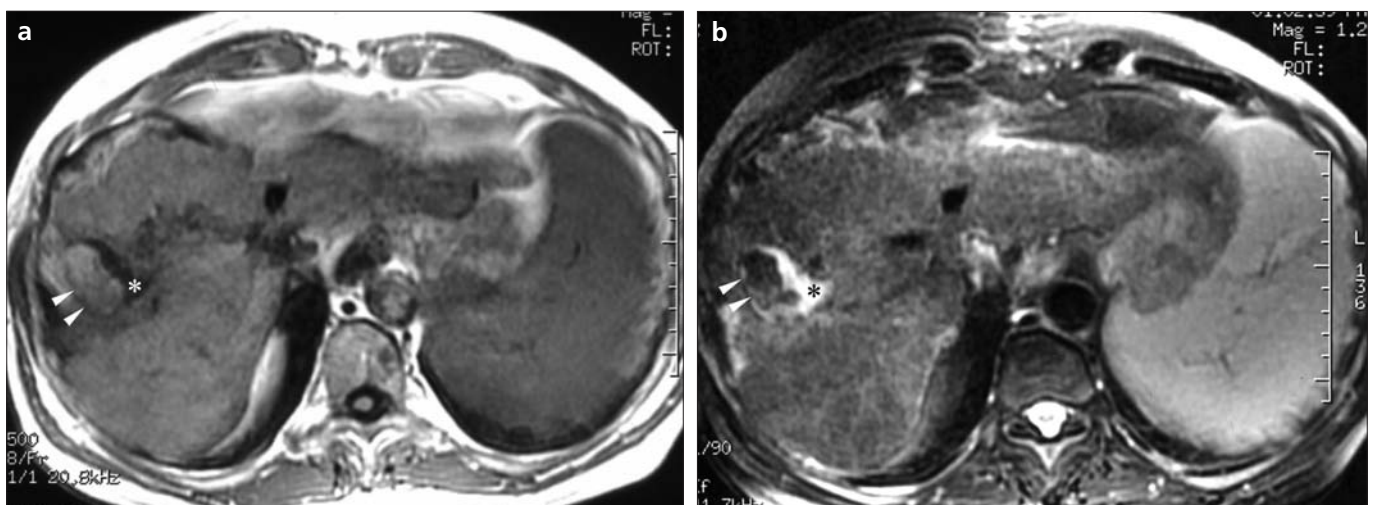

Figure 3. a, b. Axial T1- **(a)** and T2-weighted **(b)** MR images of a 73-year-old man following radiofrequency ablation therapy for hepatocellular carcinoma. In the ablation site, coagulation necrosis is typically seen as a T1-hyperintense, and T2-hypointense area *(arrowheads)*. Conversely, liquefaction necrosis appears as hypointense on T1-, and hyperintense on T2-weighted MR images *(asterisks)*.
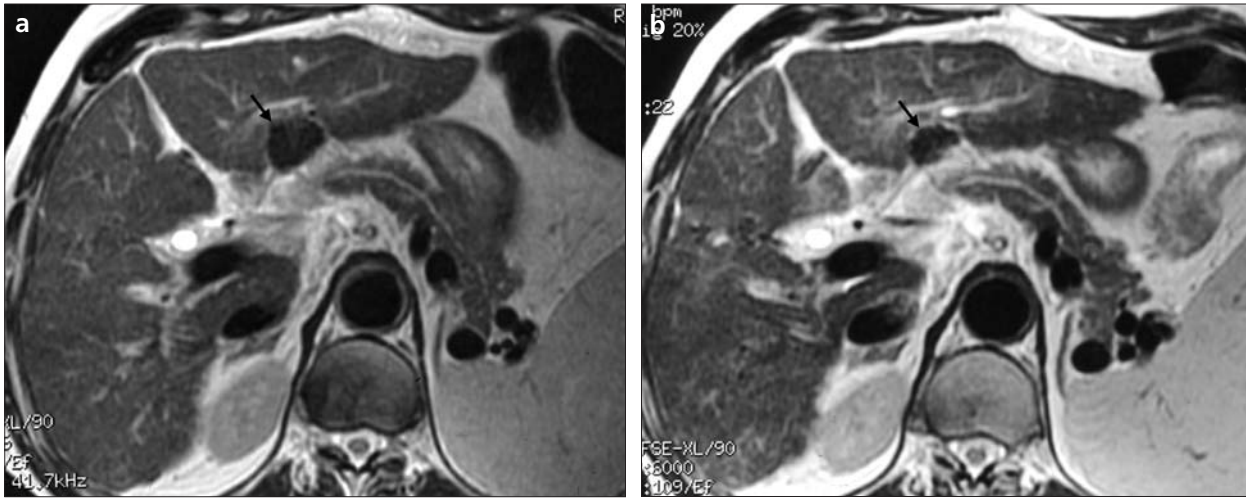
Figure 4. a, b. Sequential axial MR images **(a, b)** of a 67-year-old man following radiofrequency ablation therapy for hepatocellular carcinoma. Postablation T2-weighted MR image **(a)** shows a hypointense nodular area at segment 3 of the liver, consistent with coagulation necrosis *(arrow)*. Second T2-weighted MR image **(b)** obtained 8 months after the first MRI study shows the shrinkage of the coagulation necrosis area *(arrow)*.
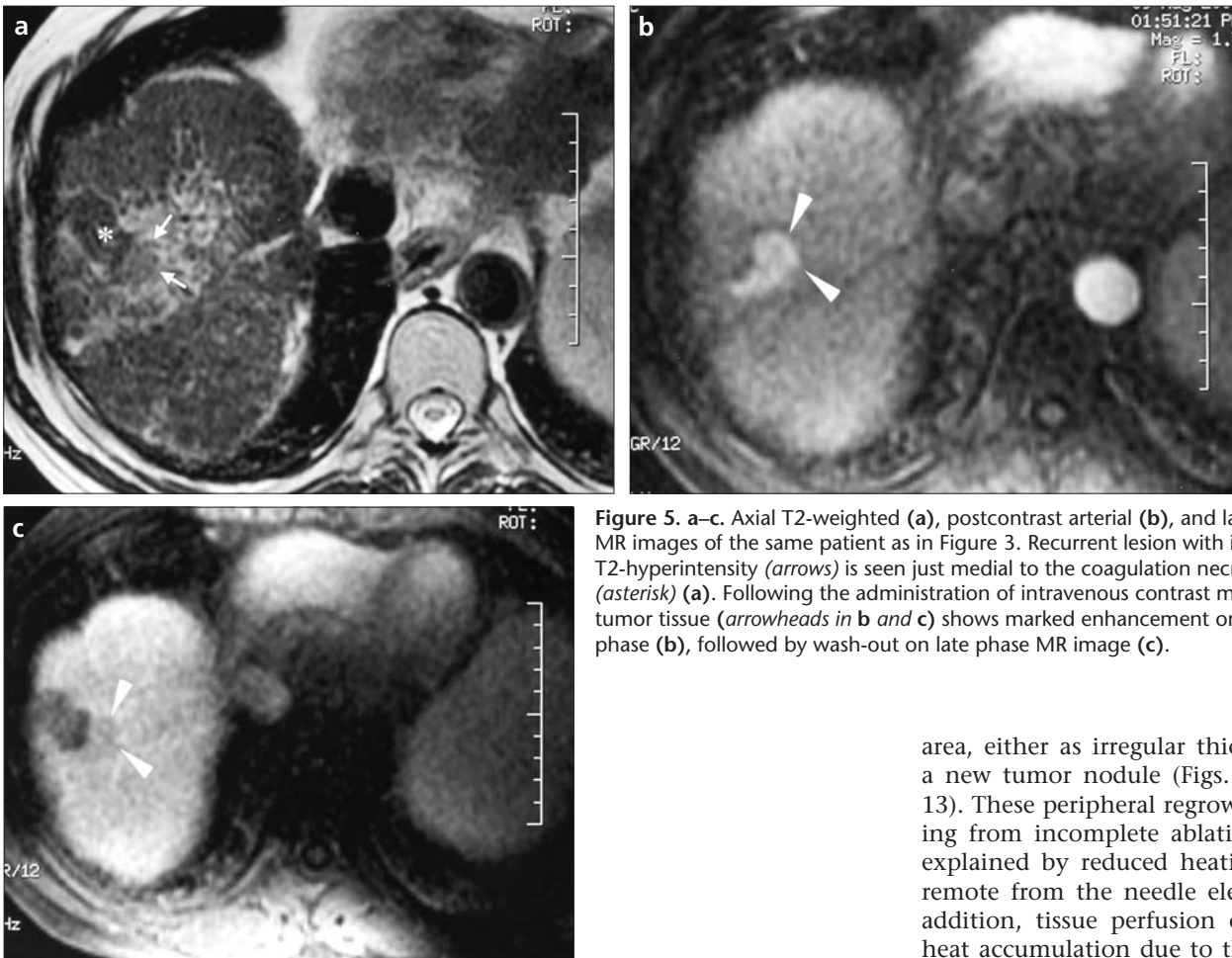

Figure 5. a–c. Axial T2-weighted **(a)**, postcontrast arterial **(b)**, and late phase **(c)** MR images of the same patient as in Figure 3. Recurrent lesion with intermediate T2-hyperintensity *(arrows)* is seen just medial to the coagulation necrosis area *(asterisk)* **(a)**. Following the administration of intravenous contrast material, tumor tissue *(arrowheads in **b** and **c**)* shows marked enhancement on arterial phase **(b)**, followed by wash-out on late phase MR image **(c)**.

perintense nodule and the hypointense background of the necrotic cavity. The residual focus or tumor recurrence usually looks like the original tumor, exhibits moderately high signal intensity on T2-weighted images (Fig. 5a), and often

shows enhancement on arterial-phase images (Fig. 5b). An increase in the size of the necrotic cavity is also another sign of recurrence (14).

Local recurrence is almost always depicted at the periphery of the necrotic

area, either as irregular thickening or a new tumor nodule (Figs. 5 a–c) (5, 13). These peripheral regrowths resulting from incomplete ablation can be explained by reduced heating that is remote from the needle electrode. In addition, tissue perfusion diminishes heat accumulation due to the cooling effect, even more markedly in tissues in contact with large vessels (heat sink phenomenon) (13).

Following RF ablation, enhancement patterns of residual or recurrent tumors on MRI are similar to CT findings (15). Chopra et al. defined three different patterns of local recurrence on follow-

up CT studies of patients with liver tumors treated with RF ablation: nodular, halo, or gross-enlargement type (16). The nodular type is characterized by a new mass on the border of the ablation cavity, protruding either internally or externally. The halo type is recognized as a prominent rim around the cavity. The gross-enlargement type is an increase in the overall tumor size compared with the previous study (16).

In a recent study concerning the follow-up imaging of the fatty HCC lesions after RF ablation, persistence of the fat content was observed at follow-up imaging in all post-ablation lesions (17). Authors claim that persistence of fat did not necessarily signify treatment failure. However, changes in fat content (increase or decrease in size) can be used as an additional criterion for the determination of treatment success (17).

In a small study of 50 tumors in 31 patients, Dromain et al. (13) found that MRI is superior to CT in detecting the early local regrowth of hepatic tumors following RF ablation. The authors suggest that the higher sensitivity of MRI over CT is mostly due to the T2-weighted images. On T2-weighted images, the high signal intensity of the residual tumor is easy to distinguish from the low signal intensity of a coagulated area (13).

The importance of T2-weighted MRI in determining the presence of complete or partial tumor ablation was also emphasized by Sironi et al. (18). They suggested that MRI is a valuable alternative to CT. Furthermore, they claimed that MRI has an advantage over CT because MRI is independent of contrast agents. Thus, although contrast-enhanced dynamic sequences are most reliable, follow-up imaging after RF ablation also can be performed using T2-weighted sequences.

Follow-up MRI studies are performed to evaluate the effectiveness of ablation, and to reveal any possible complications after ablative therapies. Although there is still no consensus regarding the timing of follow-up examinations, most centers prefer to obtain a baseline examination within the first week of the procedure primarily to detect complications or gross residual tumor that requires new intervention, and for follow-up comparison. Subsequent follow-up images are usually performed every three months for one year, and every six months thereafter (5, 10, 14). Follow-up

imaging intervals can change according to the patient's condition or the tumor type — it may be shorter in aggressive conditions (10, 14).

Complications following ablative therapies can be classified as minor and major. In the multicenter large series including 3554 RF-treated lesions reported by Livraghi et al. (11), the death rate was 0.3%, with two cases of multiorgan failure following intestinal perforation, one case of septic shock following peritonitis, one case of massive hemorrhage following tumor rupture, one case of liver failure following stenosis of the right bile duct, and one case of sudden death of unknown cause. The rate of other major complications was 2.2%. These included peritoneal hemorrhage, neoplastic seeding, intrahepatic abscesses, and intestinal perforation.

The most common minor complications are pain, skin burns, fever, nausea, dyspnea, subcutaneous and subcapsular hematoma, biloma, intraperitoneal hemorrhage not requiring surgery, pleural effusion, and pneumothorax (5).

2.b. Percutaneous ethanol injection (PEI)

PEI is a low-cost and well tolerated procedure that is performed under CT or ultrasound guidance. PEI is effective for the treatment of small, localized HCC in patients not eligible for surgery (1). In this procedure, approximately 8–10 mL absolute alcohol is percutaneously injected into the tumor in each session, under conscious sedation (3). Alcohol causes cellular dehydration, coagulative necrosis, and tissue ischemia. Generally, up to three tumors, each smaller than 5 cm, can be treated safely with PEI (1). Usually, tumors smaller than 2 cm can be ablated completely in a single session (1, 3) whereas larger tumors may require several sessions (3). Also, the high recurrence rate (up to 50% by two years) necessitates additional PEI sessions, as well as close follow-up (1, 19).

In a study by Livraghi et al., among all HCC tumors treated by either RF ablation or PEI, RF ablation resulted in a higher rate of complete necrosis (90% vs 80%) and required fewer treatment sessions than did PEI (20). On the other hand, the complication rate was found to be higher with RF ablation than with PEI (20). In a more recent systematic review published by Cho et al., RFA demonstrated significantly

improved 3-year survival in HCC patients, compared with PEI (21).

Similar to the post-treatment MRI characteristics following successful RF ablation therapy, tumors that have undergone complete necrosis after PEI usually show high signal intensity on T1-weighted and low signal intensity on T2-weighted MR images (Figs. 6, 7). Alcohol-induced necrosis is observed as a hypointense area on T2-weighted images due to cellular dehydration and protein denaturation, which result in coagulative necrosis of the tumor. By contrast, residual viable tumor tissue that persists after the PEI treatment is still of high signal intensity on T2-weighted images, similar to the pre-treatment images (22). Also a thin, regular, and peripheral enhancing rim can be observed (similar to the perilesional rim after RF treatment), which does not reflect tumor persistence, particularly when there is lymphohistiocytic infiltration (Figs. 6b, 7e) (19).

When hyperintense areas persist on T2-weighted MR images along with the usual T2-hypointensity following treatment, a definitive conclusion regarding the outcome of PEI treatment may not be made solely on the basis of the T2-weighted MR images. Liquefactive necrosis, as well as the persistent tumor tissue, can also cause T2-hyperintensity (19, 23). Thus, contrast-enhanced MRI is more reliable in evaluating the effectiveness of treatment. Unlike the non-enhancing liquefactive necrosis, contrast-enhanced T1-weighted MR images can clearly show the viable neoplastic tissue as enhancing areas within the treated lesion (Fig. 8) (19).

Catalano et al. described four different kinds of tumor recurrence on CT studies following ablative therapies (mainly after PEI) (24); tumor within the edge of the necrotic cavity (ingrowth) (Fig. 8), tumor around the cavity and in continuity with its border (outgrowth), tumor within the same segment of the necrotic cavity (spread), and tumor within different liver segments from the necrotic cavity (progression). All kinds of recurrences enhanced on arterial phase images. This categorization may also be applied to MRI studies.

3. Transcatheter arterial chemoembolization (TACE)

TACE is suitable for patients with multiple liver masses or a large tumor
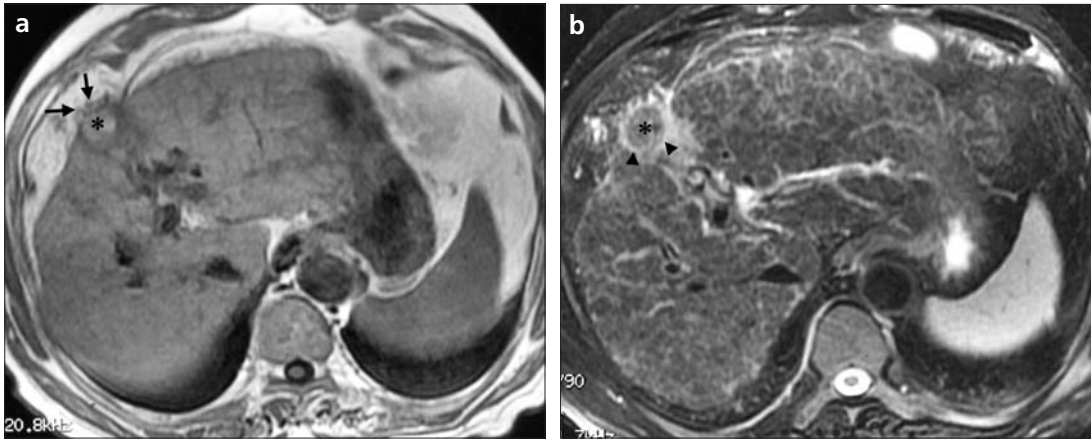
Figure 6. a, b. Axial T1- **(a)**, and T2-weighted **(b)** MR images of a 69-year-old man who had undergone multiple sessions of percutaneous ethanol injection therapy for hepatocellular carcinoma. Coagulation necrosis appears as a high signal intensity area on T1-weighted, and low signal intensity area on T2-weighted MR images *(asterisks)*. Perilesional T2-hyperintensity *(arrowheads,* **b)** consistent with edema and inflammation is also seen. Note the stranding of the neighboring extrahepatic fat tissue, due to therapeutic interventions **(***arrows,* **a)**.
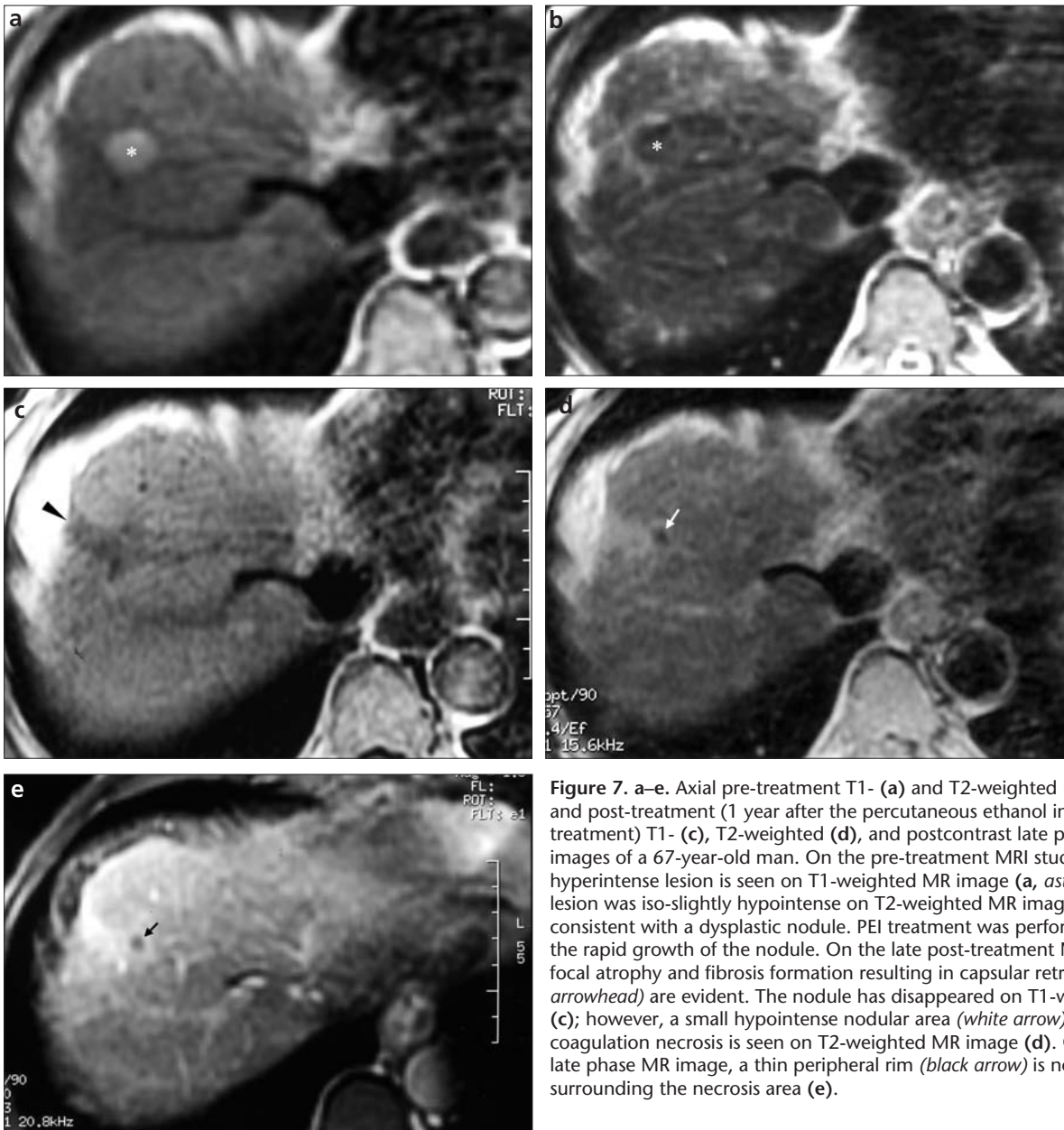

Figure 7. a–e. Axial pre-treatment T1- **(a)** and T2-weighted MR images **(b)**, and post-treatment (1 year after the percutaneous ethanol injection [PEI] treatment) T1- **(c)**, T2-weighted **(d)**, and postcontrast late phase **(e)** MR images of a 67-year-old man. On the pre-treatment MRI study, a nodular hyperintense lesion is seen on T1-weighted MR image **(a,** *asterisk***)**. This lesion was iso-slightly hypointense on T2-weighted MR images **(b,** *asterisk***)**, consistent with a dysplastic nodule. PEI treatment was performed because of the rapid growth of the nodule. On the late post-treatment MR study **(c–e)**, focal atrophy and fibrosis formation resulting in capsular retraction *(black arrowhead)* are evident. The nodule has disappeared on T1-weighted image **(c)**; however, a small hypointense nodular area *(white arrow)* consistent with coagulation necrosis is seen on T2-weighted MR image **(d)**. On postcontrast late phase MR image, a thin peripheral rim *(black arrow)* is noted, surrounding the necrosis area **(e)**.
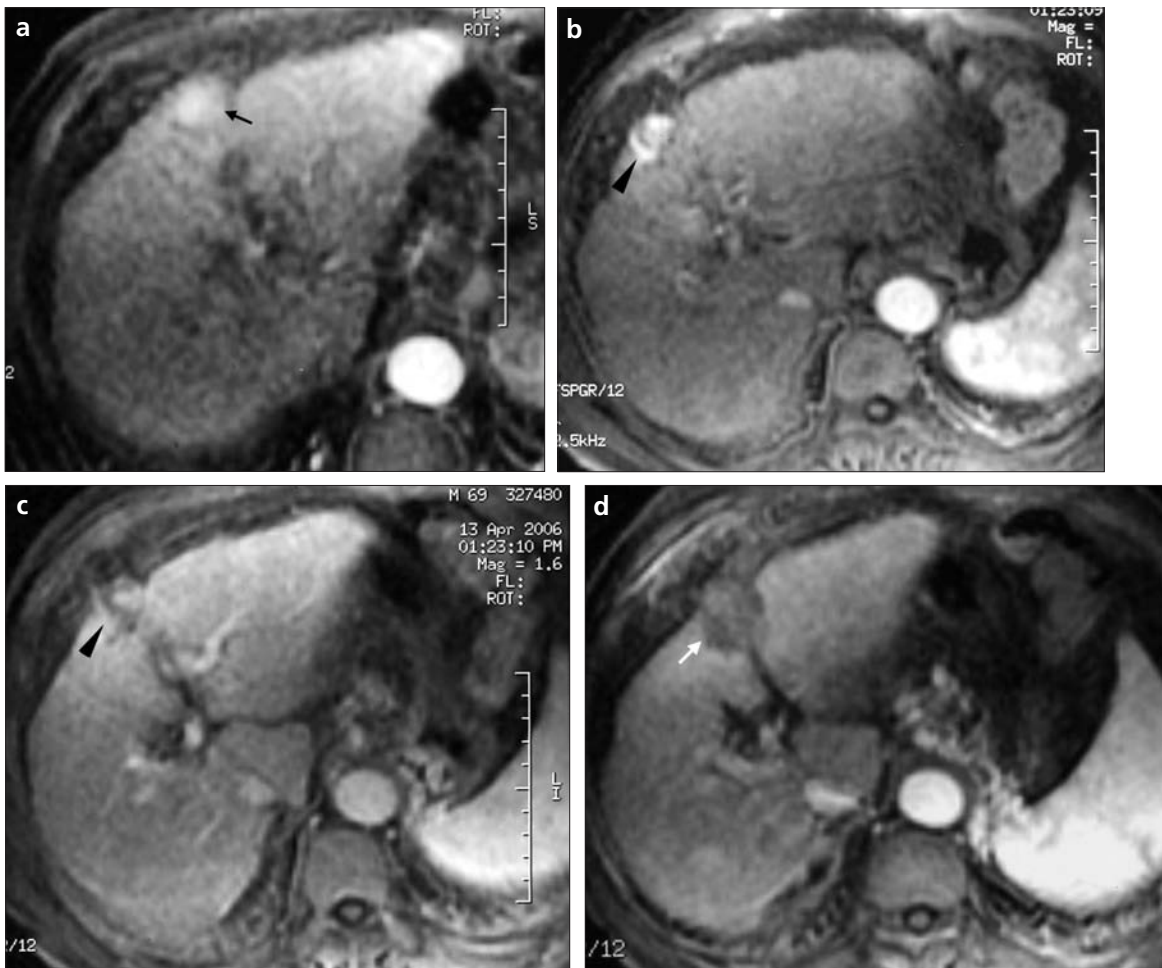
Figure 8. a–d. Axial dynamic contrast enhanced MR images of the same patient as in Figure 6, on different dates. On the first MR image **(a)** that was obtained at postcontrast arterial phase, a subcapsular enhancing nodular lesion *(black arrow)* consistent with hepatocellular carcinoma is seen, adjacent to the falciform ligament of the liver. On the post-treatment MR images following percutaneous ethanol injection (PEI) therapy, obtained at the postcontrast arterial **(b)** and late **(c)** phase, prominent heterogeneous arterial enhancement of the lesion, followed by wash-out *(arrowheads)* is shown, consistent with residual tumor. Last image obtained after a second session of PEI, at the postcontrast arterial phase **(d)** shows no enhancement indicating successful therapy *(white arrow)*.

that is not amenable to for percutaneous ablation therapy (15). It is useful in local tumor control, preventing tumor progression, prolonging survival, and controlling symptoms. It can also be used solely or in combination with other minimally invasive procedures as a neoadjuvant therapy, or prior to liver transplantation or resection (25). The main rationale for TACE is the fact that more than 80% of the blood supply of HCC is derived from the hepatic artery, in contrast to 20–30% of the blood supply of hepatic parenchyma (1, 25). Following selective catheterization, chemotherapeutic agents (usually doxorubicin or cisplatin) suspended in lipiodol (iodized oil), are injected into the feeding hepatic arteries of the tumor. This process is followed by embolizing the feeding arteries using agents such as gelatin, sponge particles, starch, col-

lagen, or autologous blood (1, 25). The purpose of embolization is to cause ischemia and to extend contact of the chemotherapeutic agent with the tumor. Tumor ischemia raises the local drug concentration, and reduces the systemic toxicity as well (25). Iodized oil serves as a carrier of chemotherapeutic agents, and is preferentially deposited in the tumor tissue, which lacks Kupffer cells, in contrast to the normal hepatic parenchyma (15). In contrast to CT imaging, the iodized oil that is used during TACE does not affect MR signal intensity (6, 15, 26).

Following TACE therapy, sufficiently treated tumors usually are replaced by necrosis (Figs. 9, 10). On T2-weighted images, the necrotic area appears moderately hypo- or isointense (Fig. 9a) (5). In addition to residual tumor, T2 hyperintensity can represent hemor-

rhage, liquefactive necrosis, or inflammatory infiltrate (6).

Similar to the necrotic area following ablative therapy, the necrotic area following TACE does not show enhancement on contrast-enhanced series (Figs. 9–11) (5, 6, 26). Thus, enhancing portions of the tumor are presumed to be viable. Residual tumor shows homogeneous or heterogeneous rapid enhancement on the arterial phase images (6). Occasionally, however, contrast-enhanced MRI cannot distinguish viable tumor cells from reactive granulation tissue. In addition, an enhancing rim that reflects either viable tumor or reactive tissue can appear on contrast-enhanced images (Fig. 11c) (6). Because of this hyperintense ring appearing in the early and late phases of dynamic series, it can be difficult to detect small residual areas located in the capsule (25). In
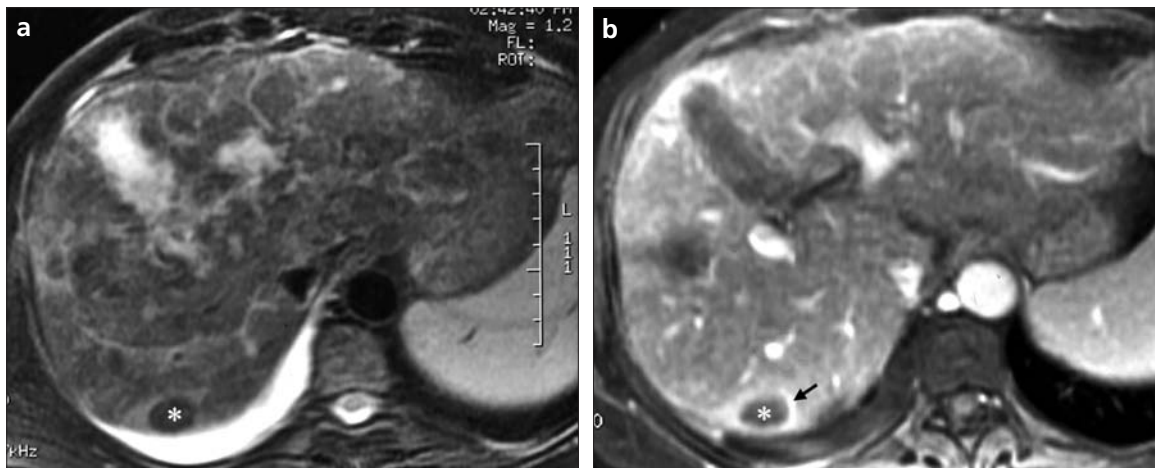
Figure 9. a, b. Axial fat-suppressed T2-weighted **(a)** and postcontrast late phase MR images of a 52-year-old woman with hepatocellular carcinoma, following transcatheter arterial chemoembolization therapy. On both sequences **(a, b)**, the necrotic area at the 7th segment of the liver appears hypointense *(asterisk)*. On the postcontrast late phase MR image **(b)** a thin enhancing rim surrounding the necrotic cavity *(arrow)* is evident; the necrotic area does not show enhancement. This enhancing rim usually represents reactive granulation tissue, rather than residual tumor.
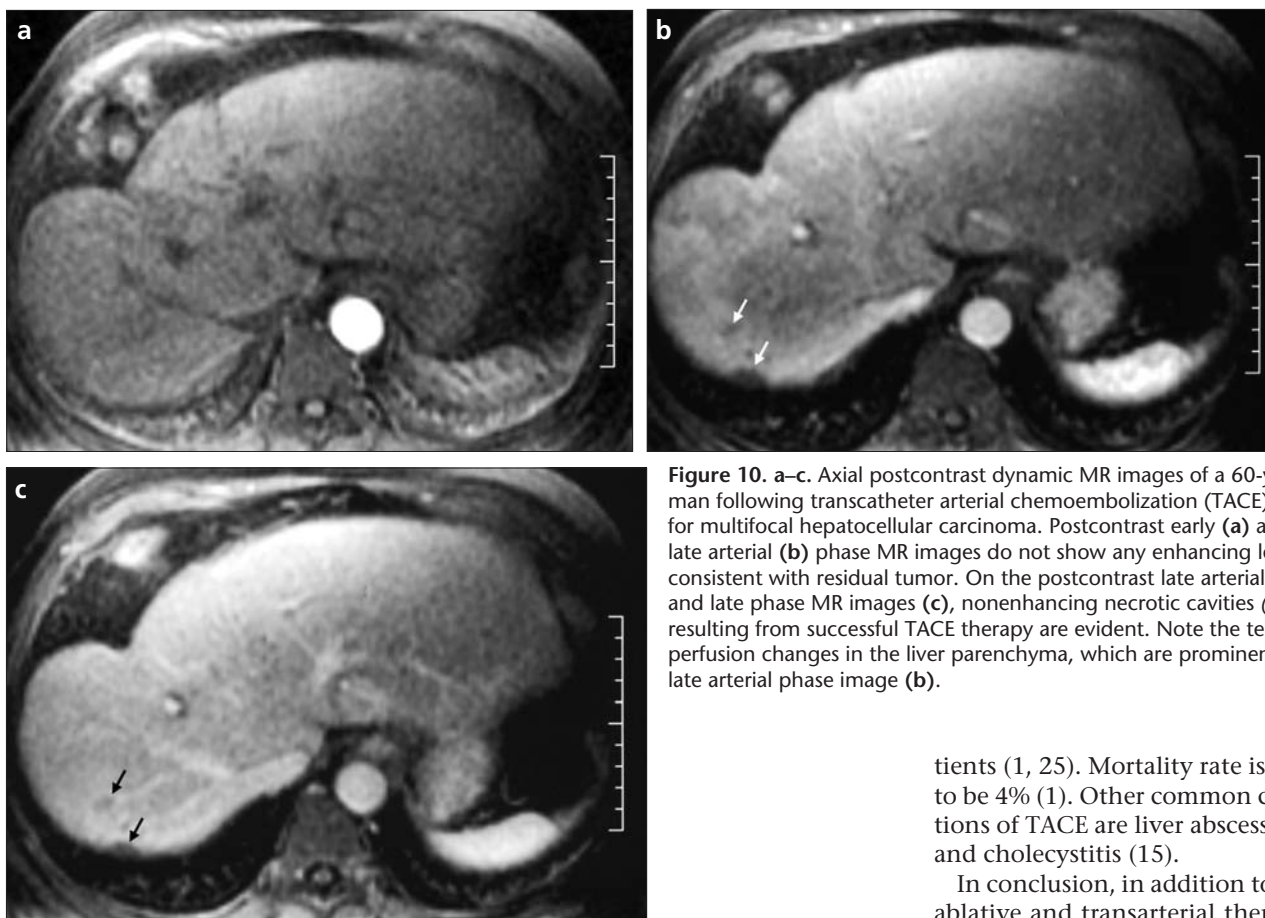

Figure 10. a–c. Axial postcontrast dynamic MR images of a 60-year-old man following transcatheter arterial chemoembolization (TACE) therapy for multifocal hepatocellular carcinoma. Postcontrast early **(a)** and late arterial **(b)** phase MR images do not show any enhancing lesion consistent with residual tumor. On the postcontrast late arterial **(b)** and late phase MR images **(c)**, nonenhancing necrotic cavities *(arrows)* resulting from successful TACE therapy are evident. Note the temporary perfusion changes in the liver parenchyma, which are prominent on the late arterial phase image **(b)**.

a recent study by Goshima et al., diffusion-weighted MRI was not found to be superior to contrast-enhanced MRI in predicting local HCC recurrence following TACE therapy (27). Thus, in these conditions, a final decision can be made only according to follow-up imaging. In general, follow-up imaging is usually performed at 4–6 weeks, and every 3–4 months thereafter (15).

The main complication of TACE is the postembolization syndrome characterized by nausea, vomiting, pain, and fever, occurring in 2–7% of patients (1, 25). Mortality rate is assumed to be 4% (1). Other common complications of TACE are liver abscess, biloma, and cholecystitis (15).

In conclusion, in addition to surgery, ablative and transarterial therapies are widely accepted options in the treatment of HCC. Although post-treatment follow-up is usually accomplished with both CT and MRI, MRI is found to be superior in detecting residual or recurrent tumors after treatment. MRI is also used for diagnosing post-treatment complications. For radiologists, familiarity with post-treatment MRI findings
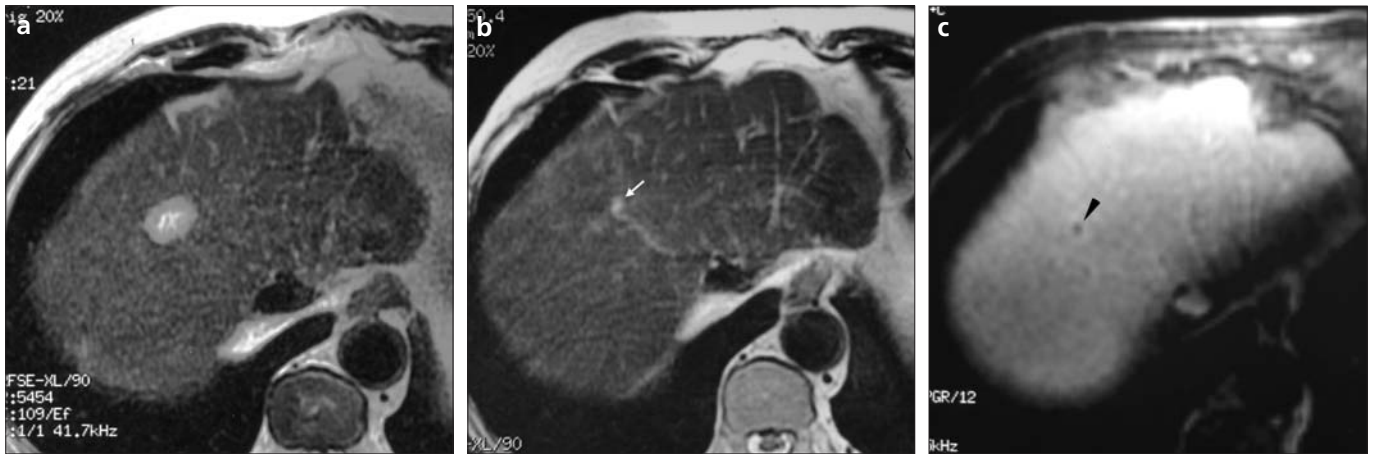
Figure 11. a–c. Axial pre- **(a)**, and post-treatment **(b, c)** MR images of a 73-year-old man with multifocal hepatocellular carcinoma, following transcatheter arterial chemoembolization therapy. Pre-treatment T2-weighted MR image **(a)** shows a nodular hyperintense focal lesion indicating hepatocellular carcinoma. On the post-treatment T2-weighted MR image **(b)**, the lesion had almost disappeared, and only a hyperintense millimetric focus is noted *(arrow)*. This millimetric lesion did not enhance on postcontrast arterial phase (not shown). On the postcontrast late phase MR image **(c)**, an enhancing rim surrounding the necrotic cavity is seen *(arrowhead)*.

is critical for the correct interpretation of these examinations and for guiding further therapies.

References

1. Cha C, DeMatteo RP, Blumgart LH. Surgery and ablative therapy for hepatocellular carcinoma. J Clin Gastroenterol 2002; 35: S130–S137.
2. Patt CH, Thuluvath PJ. Role of liver transplantation in the management of hepatocellular carcinoma. J Vasc Interv Radiol 2002; 13:S205–S210.
3. Befeler AS, Di Bisceglie AM. Hepatocellular carcinoma: diagnosis and treatment. Gastroenterology 2002; 122:1609–1619.
4. Goldberg SN, Gazelle GS, Mueller PR. Thermal ablation therapy for focal malignancy: a unified approach to underlying principles, techniques, and diagnostic imaging guidance. AJR Am J Roentgenol 2000; 174:323–331.
5. Braga L, Guller U, Semelka RC. Pre-, peri-, and post-treatment imaging of liver lesions. Radiol Clin North Am 2005; 43:915–927.
6. Vossen JA, Buijs M, Kamel IR. Assessment of tumor response on MR imaging after locoregional therapy. Tech Vasc Interv Radiol 2006; 9:125–132.
7. Goshima S, Kanematsu M, Matsuo M, et al. Early-enhancing non-neoplastic lesions on gadolinium-enhanced magnetic resonance imaging of the liver following partial hepatectomy. J Magn Reson Imaging 2004; 20:66–74.
8. Goldberg SN, Charboneau JW, Dodd GD 3rd, et al.; International Working Group on Image-Guided Tumor Ablation. Image-guided tumor ablation: proposal for standardization of terms and reporting criteria. Radiology 2003; 228:335–345.
9. Lencioni RA, Allgaier HP, Cioni D, et al. Small hepatocellular carcinoma in cirrhosis: randomized comparison of radio-frequency thermal ablation versus percutaneous ethanol injection. Radiology 2003; 228:235–240.
10. Smith S, Gillams A. Imaging appearances following thermal ablation. Clin Radiol 2008; 63:1–11.
11. Livraghi T, Solbiati L, Meloni MF, Gazelle GS, Halpern EF, Goldberg SN. Treatment of focal liver tumors with percutaneous radio-frequency ablation: complications encountered in a multicenter study. Radiology 2003; 226:441–451.
12. Goldberg SN, Gazelle GS, Compton CC, Mueller PR, Tanabe KK. Treatment of intrahepatic malignancy with radiofrequency ablation: radiologic-pathologic correlation. Cancer 2000; 88:2452–2463.
13. Dromain C, de Baere T, Elias D, et al. Hepatic tumors treated with percutaneous radio-frequency ablation: CT and MR imaging follow-up. Radiology 2002; 223:255–262.
14. Limanond P, Zimmerman P, Raman SS, Kadell BM, Lu DS. Interpretation of CT and MRI after radiofrequency ablation of hepatic malignancies. AJR Am J Roentgenol 2003; 181:1635–1640.
15. Thabet A, Kalva S, Gervais DA. Percutaneous image-guided therapy of intra-abdominal malignancy: imaging evaluation of treatment response. Abdom Imaging 2008 Nov 15 [Epub ahead of print].
16. Chopra S, Dodd GD 3rd, Chintapalli KN, Leyendecker JR, Karahan OI, Rhim H. Tumor recurrence after radiofrequency thermal ablation of hepatic tumors: spectrum of findings on dual-phase contrast-enhanced CT. AJR Am J Roentgenol 2001; 177:381–387.
17. Pupulim LF, Hakimé A, Barrau V, Abdel-Rehim M, Zappa M, Vilgrain V. Fatty hepatocellular carcinoma: radiofrequency ablation-imaging findings. Radiology 2009; 250:940–948.
18. Sironi S, Livraghi T, Meloni F, De Cobelli F, Ferrero C, Del Maschio A. Small hepatocellular carcinoma treated with percutaneous RF ablation: MR imaging follow-up. AJR Am J Roentgenol 1999; 173:1225–1229.
19. Bartolozzi C, Lencioni R, Caramella D, Mazzeo S, Ciancia EM. Treatment of hepatocellular carcinoma with percutaneous ethanol injection: evaluation with contrast-enhanced MR imaging. AJR Am J Roentgenol 1994; 162:827–831.
20. Livraghi T, Goldberg SN, Lazzaroni S, Meloni F, Solbiati L, Gazelle GS. Small hepatocellular carcinoma: treatment with radio-frequency ablation versus ethanol injection. Radiology 1999; 210:655–661.
21. Cho YK, Kim JK, Kim MY, Rhim H, Han JK. Systematic review of randomized trials for hepatocellular carcinoma treated with percutaneous ablation therapies. Hepatology 2009; 49:453–459.
22. Sironi S, Livraghi T, Angeli E, et al. Small hepatocellular carcinoma: MR follow-up of treatment with percutaneous ethanol injection. Radiology 1993; 187:119–123.
23. Lencioni R, Caramella D, Bartolozzi C. Response of hepatocellular carcinoma to percutaneous ethanol injection: CT and MR evaluation. J Comput Assist Tomogr 1993; 17:723–729.
24. Catalano O, Lobianco R, Esposito M, Siani A. Hepatocellular carcinoma recurrence after percutaneous ablation therapy: helical CT patterns. Abdom Imaging 2001; 26:375–383.
25. Vogl TJ, Naguib NN, Nour-Eldin NE, et al. Review on transarterial chemoembolization in hepatocellular carcinoma: palliative, combined, neoadjuvant, bridging, and symptomatic indications. Eur J Radiol 2008 Oct 1. [Epub ahead of print]
26. Lim HS, Jeong YY, Kang HK, Kim JK, Park JG. Imaging features of hepatocellular carcinoma after transcatheter arterial chemoembolization and radiofrequency ablation. AJR Am J Roentgenol 2006; 187: W341–349.
27. Goshima S, Kanematsu M, Kondo H, et al. Evaluating local hepatocellular carcinoma recurrence post-transcatheter arterial chemoembolization: is diffusion-weighted MRI reliable as an indicator? J Magn Reson Imaging 2008; 27:834–839.